DOI: 10.1002/ejic.200901230

Low-Temperature Synthesis of Phase-Pure 0D–1D $BaTiO_3$ Nanostructures Using $H_2Ti_3O_7$ Templates

Duk Kyu Lee,[a,b] In-Sun Cho,[a] SangWook Lee,[a] Dong Hoe Kim,[a] Hyun-Woo Shim,[c] Dong-Wan Kim,*[c] and Kug Sun Hong*[a]

Keywords: Barium / Nanostructures / Perovskite phases / Template synthesis / Titanates / Solvent effects

One-dimensional (1D) barium titanate ($BaTiO_3$) nanowires, which were uniformly covered with 0D $BaTiO_3$ nanocrystals, were synthesized by using a simple solvothermal reaction of protonated trititanate ($H_2Ti_3O_7$) nanowires with barium hydroxide octahydrate [$Ba(OH)_2{\cdot}8H_2O$] at 80 °C in ethanol/water mixed solvent systems. The compositions of the mixed solvents − the volume ratio of ethanol to deionized water − was a key controlling parameter in order to determine the phase formation and primary particle size of the 0D $BaTiO_3$ nanocrystals. Single-phase cubic perovskite $BaTiO_3$ started to form at 80 °C in a mixed solvent containing more than approximately 60 % by volume of ethanol. Field-emission scanning electron microscopy (FESEM) and high-resolution transmission electron microscopy (HRTEM) analysis revealed that the as-prepared $BaTiO_3$ retained its wire-shaped morphology with nanocrystals on the surface. Furthermore, the synthetic mechanism of the 0D-1D $BaTiO_3$ nanostructures was demonstrated in view of the dielectric tuning of the mixed solvent and the similarities between the crystal structures of $BaTiO_3$ and $H_2Ti_3O_7$.

Introduction

A ferroelectric material, $BaTiO_3$ with perovskite structures, exhibits large nonlinear optical coefficients and large dielectric constants, which are responsible for its widespread applications in the manufacturing of thermistors, multilayer/embedded capacitors, and electro-optical devices. Conventionally, barium titanate is synthesized by using the solid-state reaction method with $BaCO_3$ and TiO_2 powders,[1] which generally requires repeated mechanical mixing and high temperatures. Thus, large particle sizes, low surface areas, and irregular particle morphologies can occur.[2] Previous reports have examined the synthesis of $BaTiO_3$ nanopowders by using various methods including hydrothermal, solvothermal, microemulsion, and sol–gel methods.[3] The morphology of these powders was almost spherical (zero dimension, 0D).

Low-dimensional nanostructures can be used as nanoscale device elements and interconnects with unique properties because of their size confinement from a high aspect ratio. Therefore, many researchers have studied the synthesis of low-dimensional inorganic materials such as nanowires and nanotubes. The hydrothermal synthesis of barium titanate nanowires was previously reported. Urban et al. synthesized $BaTiO_3$ nanowires through the solution-phase decomposition of barium titanium isopropoxide in the presence of coordinating ligands at 280 °C and examined their ferroelectric properties.[4] Joshi et al. synthesized $BaTiO_3$ wires by using $Ba(OH)_2$ and TiO_2 at high pH at 170 °C.[5] The amorphous protonated titania nanoparticles are more reactive than crystallized TiO_2 and upon reaction with barium hydroxide form $BaTiO_3$ at low temperature, retaining the particle morphology of protonated titania.[6] Most of the previous reports in this area have focused on the effect of the Ba source, surfactant, pH, and solute concentration on the formation of $BaTiO_3$. However, few reports have examined the effect of the solvent.

The addition of a low dielectric medium into the aqueous solution can alter the thermodynamics of the reaction system and the nucleation kinetics, which reduces the particle size and size distribution of the resulting particles.[7] However, these reports have mostly focused on the synthesis of binary compounds, such as ZrO_2 or TiO_2 etc. In this work, 0D–1D $BaTiO_3$ nanostructures were synthesized by using $Ba(OH)_2{\cdot}8H_2O$ and $H_2Ti_3O_7$ nanowires as templates in an ethanol/water mixed solvent at a low temperature around 80 °C. The effect of the volume ratio of ethanol to water on

[a] Department of Materials Science & Engineering, Seoul National University,
Seoul 151-744, South Korea
Fax: +82-2-886-4156
E-mail: kshongss@plaza.snu.ac.kr
[b] Ceramic Research & Development division, Dongil Technology Ltd,
Hwasung 445-854, Korea
[c] Department of Materials Science & Engineering, Ajou University,
Suwon 443-749, South Korea
Fax: +82-31-219-1612
E-mail: dwkim@ajou.ac.kr

Supporting information for this article is available on the WWW under http://dx.doi.org/10.1002/ejic.200901230.

the nucleation and the morphology of a prepared $BaTiO_3$ was examined with respect to the dielectric constant of the mixed solvent and the mechanism of formation of the $BaTiO_3$ phase.

Results and Discussion

Figure 1 shows the powder XRD patterns and the FESEM images of the $BaTiO_3$ (hereafter BT) nanostructures for various reaction times in the mixed water/ethanol solvent with 60% ethanol by volume (hereafter E6H4) at 80 °C. In Figure 1a, a BT phase appeared after a reaction time of 3 h and increased with the reaction time.

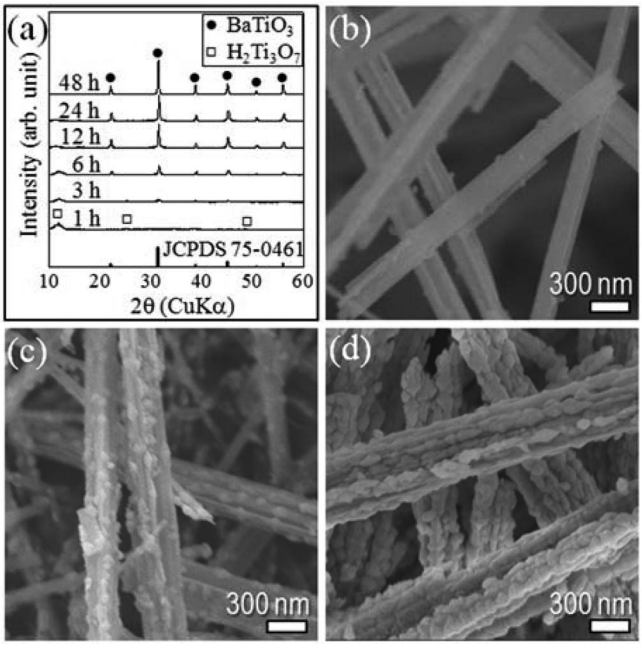

Figure 1. (a) XRD patterns of the powders prepared after various reaction times in the mixed solvent with 60 vol.-% ethanol at 80 °C. Typical FESEM images of the powders taken after reaction times of (b) 1 h, (c) 6 h, and (d) 48 h.

The powders obtained after 48 h were BT with a cubic perovskite structure (JCPDS card no. 75-0461), and a secondary phase was not present. Figure 1b–d shows the typical FESEM images of the powders prepared after reaction times of 1, 6, and 48 h, respectively. The nanoparticles were generated on the surface of the $H_2Ti_3O_7$ (hereafter HTO) wires at the beginning of the reaction, and the size and density of the nanoparticles increased over time. The entire surface was fully covered with particles, and the wire-shaped morphology was retained after the formation of the BT phase was complete.

These results were confirmed by the TEM images of each powder in Figure 2. Although the as-synthesized HTO nanowires had a smooth surface, single nanoparticles were distributed on the surface of the individual HTO nanowire after 1 h (Figure 2a). As the reaction time was increased, larger faceted nanoparticles anchored onto the surface of the nanowire (Figure 2b), and finally a 0D–1D heterostructured nanowire with high density nanoparticles resulted (Figure 2c). A similar morphology with fine $BaTiO_3$ particles attached on the surface of the fibrous $BaTiO_3$ has been reported.[8,9] In these previous works, the powders were prepared by using a hydrothermal process (not in mixed solvents) at temperatures over 150 °C with the use of protonated titanate precursors, and the morphological evolution of the powders was closely dependent on the concentration of $Ba(OH)_2$ and the reaction temperature.

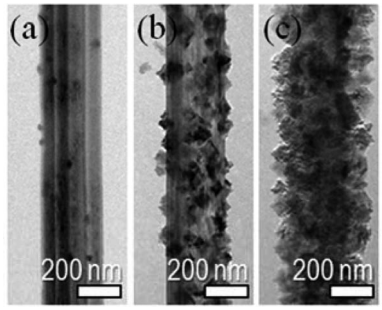

Figure 2. TEM images of the powders prepared in E6H4 at 80 °C after reaction times of (a) 1 h, (b) 6 h, and (c) 48 h.

For nanomaterials synthesis using a mixed solvent, a precipitation process, such as the addition of a low dielectric medium into an aqueous solution, can be employed to reduce the particle size and the size distribution by altering the thermodynamics of the reaction system and the nucleation kinetics. Typical FESEM images of the powders prepared after 48 h at 80 °C in pure water (E0H10), 40% (E4H6), 60% (E6H4), and 80% (E8H2) mixed solvents, and pure ethanol (E10H0) are separately shown in Figure 3. Only the E6H4 and E8H2 powders exhibited 0D–1D nanostructures, whereas the other powders retained the 1D wire-like morphology of the precursor HTO without any adjoined nanoparticles.

These FESEM observations were consistent with the XRD analysis (Figure 4). In addition, a cubic $BaTiO_3$ structure can be distinguished from a tetragonal structure with a (200) peak around 45° of 2θ.[10] The E6H4 and E8H2 powders had only one symmetric (200) peak, indicating a phase-pure cubic structure, as shown in the high-resolution XRD patterns of the inset of Figure 4. Furthermore, the formation of phase-pure 0D–1D $BaTiO_3$ nanostructures can be confirmed by detailed TEM observations of the cross-sectional core regions of an individual E6H4 particle processed by using focused ion beam manipulation (Figures S1–S3, Supporting Information).

Although the BT phase did not form in pure ethanol because of the insolubility of $Ba(OH)_2 \cdot 8H_2O$, the BT phase started to generate at low temperature, 80 °C, when the ethanol concentration was more than 60 vol.-% in the mixed solvent, which was closely related to the low dielectric constant (ε) of each solvent ($\varepsilon_{EtoH} = 25$, $\varepsilon_{water} = 80$).[11] A solvent with a low dielectric constant makes the solution more supersaturated, which can increase the nucleation rate.[12]

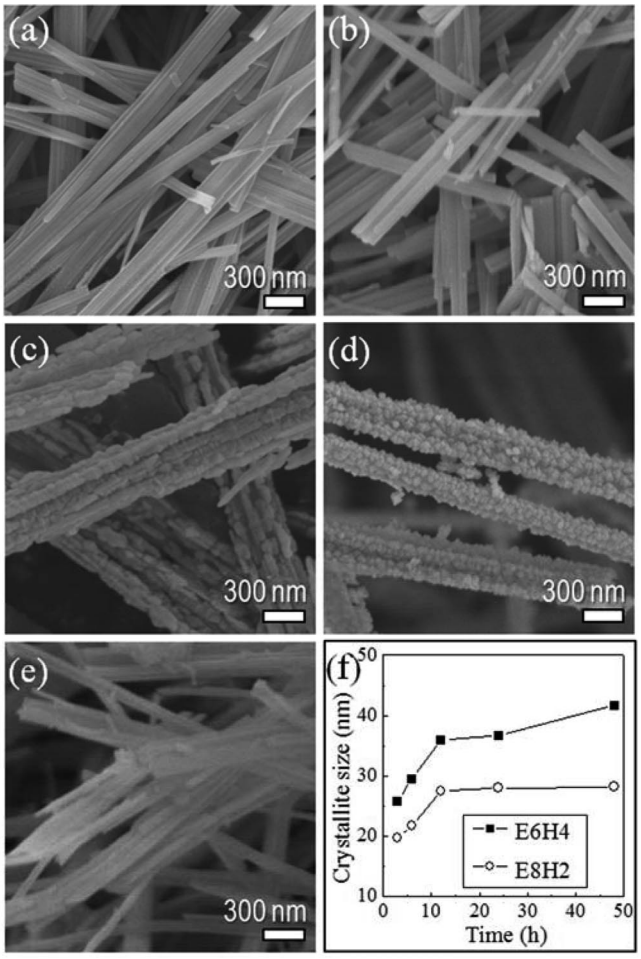

Figure 3. FESEM images of the powder prepared after 48 h at 80 °C for various ratios of mixed solvent: (a) E0H10, (b) E4H6, (c) E6H4, (d) E8H2, and (e) E10H0; (f) crystallite size of the E6H4 and E8H2 samples vs. reaction time.

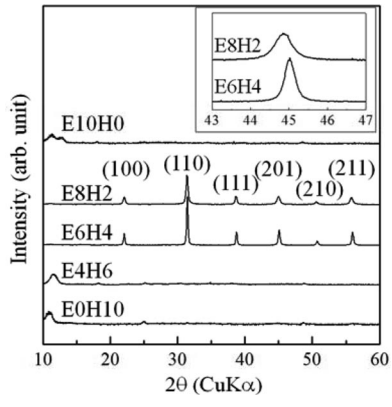

Figure 4. XRD patterns of the powders prepared after 48 h at 80 °C for different mixed solvent ratios. Inset shows the high-resolution XRD patterns around the (200) reflection peak of the E6H4 and E8H2 powders indicating the single cubic phase.

Theoretically, the dependence of the particle radius (r) on the ε of the solution can be expressed by using the electrostatic model, and the relationship between supersaturation and r can be expressed by using the Kelvin equation:[13]

$$\frac{1}{r} = A + \frac{B}{\varepsilon}$$

where $A = \frac{kT\rho}{2m\gamma} \ln C$, $B = \frac{\rho z_+ z_- e^2}{8\pi m\gamma\varepsilon_0 (r_+ + r_-)}$

where k is the Boltzmann's constant; T is the temperature in Kelvin; ρ, m, and C are the density, weight, and concentration of the solute molecule, respectively; γ is the interfacial energy between the solute and solution; the symbols r_+ and r_- represent the radii of charged z_+ and z_- ions, respectively; e and ε_0 represent the elementary charge and the dielectric constant in vacuo, respectively.

For homogeneously mixed alkyl alcohol and water solvent systems, the values of A and B can be regarded as constants. Therefore, the change in supersaturation, caused by changing the dielectric constant of the mixed solvent, can clearly affect both the nucleation rate and the particle size remarkably, which coincided with the low-temperature synthesis of BT using the mixed solvent systems and the difference in the particle size between the E6H4 and E8H2 samples (Figures 3 and 4). Additionally, from the calculation of the half-width of the XRD peaks for the BT (110) plane by using Sherrer's equation (Figure 3f), we confirmed that the primary particle size of E6H4 was larger than that of E2H8 regardless of the reaction time.

TEM and HRTEM of the powder at the initial reaction stage were examined to determine the nucleation and growth mechanisms for the formation of the 0D–1D BT nanostructures. Figure 5a shows an evident 0D–1D nanostructure for the powder prepared after 6 h reaction. From the magnified bright-field TEM image of the area marked with a square in Figure 5a, an as-formed nanocrystal was clearly interconnected onto the adjoining wire backbone (Figure 5b). As expected, the fast Fourier transform for the nanocrystal and nanowire regions corresponded to the BT and HTO phases, respectively (Figure 5c and d). These phases of the nanocrystal and wire were also confirmed in another 0D–1D nanostructured powder (Figure S4, Supporting Information).

More interestingly, the interplanar distances of d_{002} (0.200 nm) in BT and d_{020} (0.195 nm) in HTO were very similar in the HRTEM image near the interface region (Figure 5e). In Figure 5f, both BT and HTO had TiO_6 octahedral frameworks, and the spacings of lattice fringes, d_{001} in BT and d_{010} in HTO, were 0.400 and 0.376 nm, respectively, which were calculated from the reported crystallographic data. These results closely matched the measured values based on the HRTEM image in Figure 5e. The low interfacial lattice mismatch between BT and HTO could lower the heteronucleation energy barrier required for the growth of the BT nanocrystals.[14] Therefore, the oriented arrangement of the $BaTiO_3$ nanocrystals onto the surface of HTO was possible without any appreciable aggregation and was closely related to the formation of faceted BT particles rather than spherical ones as well as the retention of the 1D wire motif of HTO in Figure 2.

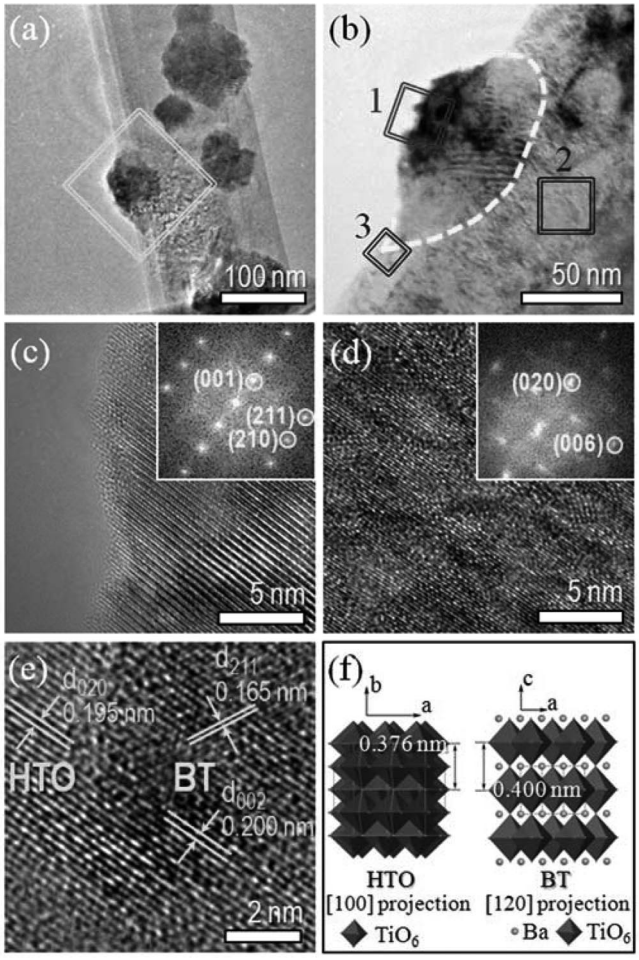

Figure 5. (a) Typical TEM image of the E6H4 powder prepared after 6 h at 80 °C; (b) magnified TEM image of the area marked with a square in (a); magnified HRTEM images of the area marked by (c) 1, (d) 2, and (e) 3 in (b); (f) schematic representation of the HTO and BT crystal structure using the TiO_6 octahedral frameworks.

Starikova et al. reported the crystalline rectangular plates or thin needles as the interaction products of $Ba(OH)_2$ or BaO with methanol.[15] It has also been reported that highly crystalline $BaTiO_3$ nanoparticles were synthesized in an aprotic acetophenone solvent at low temperature through formation of intermediate derivatives of metals.[16] In this work, a topochemical reaction process can be proposed for the formation mechanism of the 0D–1D titanate ($BaTiO_3$, $SrTiO_3$, $PbTiO_3$, and TiO_2) nanostructures during the hydrothermal process.[8,17] In the early stage of the reaction, the Ba^{2+} species (or intermediate derivatives of barium metals) in the solution reacted with the HTO nanowires that were locally dissolved at the interface and in situ precipitated to BT nanocrystals. This process was possible even at a low temperature, ca. 80 °C, because of the supersaturation caused by the lowered dielectric constant of the mixed solvent. Additionally, this process was coupled with a topochemical reaction based on the similar crystallographic features of BT and HTO. The propagation of the reaction was expected to occur from the front of the HTO to the interior until the entire HTO wires were transformed into BT through reaction with barium ions that diffused during the growth of the outer BT nanocrysals, finally yielding the phase-pure 0D–1D BT nanostructures. As described above, the low interfacial lattice mismatch between BT and HTO might have enabled complete conversion while maintaining the initial 1D wire morphology.

Conclusions

In summary, single-phase 0D–1D BT nanostructures were synthesized under simple solvothermal reaction conditions at a relatively low temperature, 80 °C, in an ethanol/water mixed solvent. The presence of ethanol provided the low-temperature nucleation of BT as well as the modulation of its particle size by decreasing the dielectric constant of the solvent. The details of the nucleation and transformation mechanism of the BT heteronanostructure were represented by using a topochemical reaction based on the close correlation between the BT and HTO crystal structures.

Experimental Section

The $H_2Ti_3O_7$ precursor was synthesized using a previously published procedure,[18] except for the molar concentration of TiO_2 used. In this study, 1.5 g of TiO_2 (Anatase, 99.9%, High Purity Chemicals) was dispersed in 300 mL of 10 M NaOH (High Purity Chemicals) aqueous solution. The solution was stirred by using a magnetic bar, sonicated for 30 min to break the TiO_2 agglomerates, and autoclaved for 48 h at 180 °C. After the hydrothermal treatment, the product was washed with distilled water and aged in an aqueous solution of 0.1 M HCl for 24 h at room temperature for full-ion exchange from Na^+ to H^+. The treated powders were filtered and washed with distilled water repeatedly until a pH near 7 was reached, and then the powders were dried in a frozen dryer.

Barium titanate was prepared by using a simple wet chemical route. Barium hydroxide octahydrate [$Ba(OH)_2{\cdot}8H_2O$, 98% Aldrich] was dissolved in distilled water, and prepared HTO was added to a beaker containing ethanol and sonicated for 20 min to break the agglomeration. The volume ratio of ethanol to distilled water was varied from 0 to 100%, and the molar ratio of Ba^{2+} to Ti^{4+} was 1.1. Two prepared solutions were mixed in a glass bottle with a cap and stirred magnetically for 30 min. The bottle was placed into a water bath at 80 °C and stirred for an adequate amount of time (1–48 h). After each reaction was complete, the resulting products were washed with 0.1 M formic acid to eliminate residual $BaCO_3$ and then washed with distilled water (3×). The final product was dried in a frozen dryer for 48 h for further characterization.

The crystal structure of the prepared powders was analyzed by using an X-ray diffractometer (M18XHF-SRA, MAC Science Co.). The microstructures and morphologies of the as-prepared powders were observed by using a field-emission scanning electron microscope (FESEM, JSM-6330F, JEOL) and a high-resolution transmission electron microscope (HRTEM, JEM-3000F, JEOL).

Supporting Information (see footnote on the first page of this article): Additional FESEM and TEM images.

Acknowledgments

This work was co-supported by a grant from the Center for Advanced Materials Processing (CAMP) of the 21st Century Frontier

R&D Program funded by the Ministry of Commerce, Industry and Energy (MOCIE), Republic of Korea and the National Research Foundation of Korea (NRF), Korea government (MEST) (No. 2009-0082544).

[1] M. C. B. Lopez, G. Fourlaris, B. Rand, F. L. Riley, *J. Am. Ceram. Soc.* **1999**, *82*, 1777–1786.

[2] I. Maclaren, C. B. Ponton, *J. Eur. Ceram. Soc.* **2000**, *20*, 1267–1275.

[3] a) H. Xu, L. Gao, *Mater. Lett.* **2004**, *58*, 1582–1586; b) D. Chen, K. Jiao, *J. Am. Ceram. Soc.* **2000**, *83*, 2637–2639; c) A. J. Zarur, J. Y. Ying, *Nature* **2000**, *403*, 65–67; d) W. Luan, L. Gao, *Ceram. Int.* **2001**, *27*, 645–648; e) D. L. Segal, *J. Non-Cryst. Solids* **1984**, *63*, 183–191.

[4] J. J. Urban, J. E. Spanier, L. Ouyang, W. S. Yun, H. K. Park, *Adv. Mater.* **2003**, *15*, 423–426.

[5] U. A. Joshi, J. S. Lee, *Small* **2005**, *1*, 1172–1176.

[6] M. Klee, *J. Mater. Sci. Lett.* **1989**, *8*, 985–988.

[7] a) M. Z. C. Hu, E. A. Payzant, C. H. Byers, *J. Colloid Interface Sci.* **2000**, *222*, 20–36; b) C. S. Fang, Y. W. Chen, *Mater. Chem. Phys.* **2003**, *78*, 739–745.

[8] Q. Feng, K. Yanagisawa, N. Yamasaki, *Adv. High Pressure Res.* **2001**, *20*, 149–154.

[9] Y. Li, X. P. Gao, G. R. Li, G. L. Pan, T. Y. Yan, H. Y. Zhu, *J. Phys. Chem. C* **2009**, *113*, 4386–4394.

[10] G. Arit, G. With, *J. Appl. Phys.* **1985**, *58*, 1619–1625.

[11] S. M. Puranik, A. C. Kumbharkhane, S. C. Mehrotra, *J. Mol. Liq.* **1994**, *59*, 173–177.

[12] a) J. N. Israelachvili, *Intermolecular and Surface Forces*, Academic Press, London, **1992**; b) A. S. Myerson, *Molecular Modeling Applications in Crystallization*, Cambridge University Press, Cambridge, **1999**.

[13] a) H. I. Chen, H. Y. Chang, *Colloid Surface A* **2004**, *242*, 61–69; b) G. Cao, *Nanostructures and Nanomaterials*, Imperial College Press, Singapore, **2004**.

[14] D. F. Zhang, L. D. Sun, C. J. Jia, Z. G. Yan, L. P. You, C. H. Yan, *J. Am. Chem. Soc.* **2005**, *127*, 13492–13493.

[15] Z. A. Starikova, V. G. Kessler, N. Y. Turova, I. A. Dantsker, A. P. Bobyljov, A. S. Mitiaev, *Polyhedron* **2006**, *25*, 2401–2406.

[16] R. Pazik, R. Tekoriute, S. Hakansson, R. Wiglusz, W. Strek, G. A. Seisenbaeva, Y. K. Gun′ko, V. G. Kessler, *Chem. Eur. J.* **2009**, *15*, 6820–6826.

[17] a) H. Y. Zhu, X. P. Gao, Y. Lan, D. Y. Song, Y. X. Xi, J. C. Zhao, *J. Am. Chem. Soc.* **2004**, *126*, 8380–8381; b) Y. Mao, S. S. Wong, *J. Am. Chem. Soc.* **2006**, *128*, 8217–8226; c) Q. Fing, M. Hirasawa, K. Yanagisawa, *Chem. Mater.* **2001**, *13*, 290–296; d) N. Bao, L. Shen, G. Srinivasan, K. Yanagisawa, A. Gupta, *J. Phys. Chem. C* **2008**, *112*, 8634–8642; e) Y. Ohara, K. Koumoto, T. Shimizu, H. Yanagida, *J. Mater. Sci.* **1995**, *30*, 263–266.

[18] Y. Wang, G. Du, H. Liu, D. Liu, S. Qin, N. Wang, C. Hu, X. Tao, J. Jiao, J. Wang, Z. L. Wang, *Adv. Funct. Mater.* **2008**, *18*, 1131–1137.

Received: December 21, 2009
Published Online: February 16, 2010

